Flexible Robust Adaptive Beamforming Method With Null Widening

Ziwei Liu, Shanshan Zhao, Chen Zhang, and Gengxin Zhang

***Abstract*—The nonstationarity of interferences and array errors may bring fatal degradation to the interference cancellation performance of an adaptive beamformer. Covariance matrix tapering (CMT) can produce wide troughs in receiving pattern and becomes a promising solution. However, not only the full adaption methods but also the robust sidelobe canceller widen all nulls symmetrically to the original directions of arrival (DOAs) with the same width. In fact, in most cases, the adaptive pattern does not need symmetrical and equivalent-width nulls since it is of little possibility that different interference poses the same nonstationarity. To cover the worst nonstationarity, traditional CMT methods need to produce a widest null and will suffer a waste of degrees of freedom (DOFs). In this paper, a flexible method for null widening is proposed which can produce wide null with different desired width and asymmetry. The asymmetry is developed from the spatial asymmetrical interference cluster, and the unequal null width is produced by disturbing different interference space with different tapering matrix. Computer simulation result corroborate the feasibility and merits of the proposed method.**

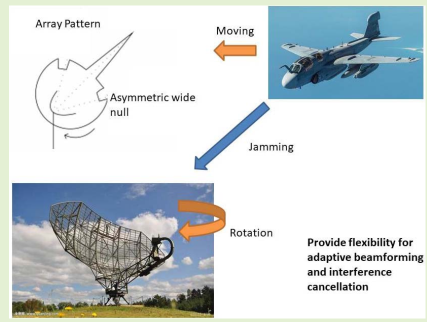

***Index Terms*—Subspace extraction, null widening, covariance matrix taper (CMT), adaptive beamforming.**

I. Introduction

ADAPTIVE beamforming, or named smart antenna techniques, has been widely used in contemporary radar and communication systems [1]–[3]. It can achieve spatial accumulation and filtering simultaneously to gain signals from the interested direction and attenuate undesired signals.

Basic steps of an adaptive beamforming algorithm consist of training weights and applying beamformer. Most algorithms hold under a potential assumption that the training samples, usually named snapshots, contain the same signals' and interferences' characteristics with that in the applied data. However, in real system, interferences may present nonstationary spatial structures which makes a characteristic mismatching between snapshots and the applied data. Taking radar as a typical example, the nonstationarity may be caused by time-varying propagation path, such as the dynamic reflection path from the ionosphere for the skywave over-the-horizon radar [4], [5], or the relative motion between the receiving antenna and interference resources, e.g. mechanical rotation of the receiving array [6]. The mismatching makes beamforming algorithms be invalid since interferences in the applied data may not fall into the sharp null trained by snapshots.

Limited by the system computational burden, it is preferred to widen the sharp null in the receiving pattern instead of updating adaptive weights frequently. A method called binary-point constraint based null widening method was proposed in [7]. But it can just afford relative narrow null width since it indeed puts two fictitious interferences around the receiving interference. Semidefinite optimization was also used for null widening [8]. It optimizes the power response around desired directions in the adaptive pattern to generate a flat null. However, it needs heavy computation costs and cannot control the phase response. A new method based on spatial spectrum reconstruction was proposed [9]. This null widening method indeed reconstructs the whole receiving covariance matrix. However, the complicated direction of arrival (DOA) estimation and reconstruction processing limits its application in real systems.

Except for the above-mentioned methods, covariance matrix taper (CMT) methods draw large amounts of attentions and

Manuscript received January 19, 2021; accepted February 14, 2021. Date of publication February 19, 2021; date of current version April 5, 2021. This work was supported in part by the National Natural Science Foundation of China under Grant 61801445, Grant 61801233, and Grant 61901230; in part by the Natural Science Foundation of Jiangsu Province under Grant BK20170911; and in part by the NUPTSF under Grant NY219011. The associate editor coordinating the review of this article and approving it for publication was Dr. Michail Antoniou. *(Corresponding author: Shanshan Zhao.)*

Ziwei Liu, Chen Zhang, and Gengxin Zhang are with the Telecommunication and Networks National Engineering Research Center, College of Telecommunications and Information Engineering, Nanjing University of Posts and Telecommunications, Nanjing 210003, China (e-mail: liuziwei89@163.com; zhangchen@njupt.edu.cn; 455613536@qq.com).

Shanshan Zhao is with the College of Electronic and Optical Engineering, Nanjing University of Posts and Telecommunications, Nanjing 210023, China (e-mail: zhaoshanshan025@163.com).

Digital Object Identifier 10.1109/JSEN.2021.3060510

are famous for its robustness and convenience. In 1995, this methodology was first proposed by Mailloux [10] and Zatman [11], individually. Guerci unified these two methods and named it as the famous CMT method in [12]. Following the CMT structure, researchers proposed much further works. The method proposed in [13] used a normal distribution to describe the random disturbing variable. Liang *et. al.* applied the CMT method to the near-field beamforming problem and obtain a robust adaptive beamformer [14]. Instead of linear or plain array, a CMT method for circular array was proposed in [15].

Regular CMT-class methods do provide excellent performance. But it must pay the price of costing more Degrees of freedom (DOFs), which is the essential “resources” for adaptive beamforming methods [16], [17]. Researchers have proven that the DOF cost is proportional to the null width and aperture of the array [18]. Based on this fact, some work was published on the sidelobe canceller [19], [20] and partial adaptive beamformer [21]–[23] to reduce the necessary computational burden by applying CMT methods under an low-complexity beamformer. However, for a fixed null width and array aperture, it is of little possibility to reduce the necessary DOF. The most effective way to save the DOF is to design the most suitable wide null flexibly for each interference source. In fact, the flexibility of CMT methods has been ignored for a long time. The flexibility consists of two part of contents: null width and location. Existing CMT methods widen all nulls to wider nulls with the same width (measured in cosine) and symmetric to the original nulls. This operation may not waste DOFs only under the assumption that all interference sources contain the same symmetric nonstationarity. In real scenarios, it is hard to meet such an ideal and strict condition. To cover the arbitrary nonstationarity, all nulls must be widened with the largest width, resulting in a waste of DOFs. Recently, a CMT-based method was proposed to produce asymmetrical nulls [6]. However, only discrete-form solution was derived. A continuous form will consolidate its application.

In this paper, a flexible CMT based method is proposed. The main merit is that both the width and the null location can be controlled for each interference source. The proposed method comes from the Mailloux’s methodology. Fictitious interference sources are introduced into snapshots. Different from regular CMT methods, the fictitious sources are placed individually and asymmetrically around each source as desired to derive the most suitable null. The individually widening operation is achieved by disturbing the principle component of each interference source, while asymmetrically widening operation depends on the asymmetrical fictitious interference clusters. The whole procedure is concluded and the closed-form formulations of the proposed method are derived. Simulation results show the effectiveness of the proposed method.

The rest of paper is organised as follows. The signal model and regular CMT method is given in Section II. The proposed method is described in Section III, including derivations and the procedure. Some simulation results are shown in Section IV and the conclusion is drawn in Section V.

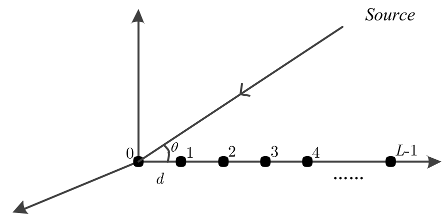

Fig. 1. Diagram of ULA.

II. Signal Model and Regular CMT

Without loss of generality, the whole receiving array consisting of a uniform linear array (ULA) with L linear equispaced omnidirectional sensors is shown in Fig.1. All sensors are assumed to be placed on axis y. The impacting cone angle is written as θ.

In our work, only narrow band signals are considered. Suppose the mainlobe of the array is steering to the desired direction θ_0 and Q narrow band interferences impacting the array from directions $\theta_q, q = 1, 2, \cdots, Q$, respectively. In a certain moment, the sampled receiving data $\boldsymbol{X}(k)$ can be modeled as

$$\boldsymbol{X}(k) = \boldsymbol{A}\boldsymbol{S}(k) + \boldsymbol{N}(k) \tag{1}$$

where $\boldsymbol{X}(k) = [x_1(k), x_2(k), \cdots, x_L(k)]^T$ is the receiving data. Matrix $\boldsymbol{A} = \left[\boldsymbol{a}(\theta_0), \boldsymbol{a}(\theta_1), \boldsymbol{a}(\theta_2), \cdots, \boldsymbol{a}(\theta_Q)\right]$ is the manifold matrix with the steering vectors in it. Steering vector $\boldsymbol{a}(\theta)$ is

$$\boldsymbol{a}(\theta) = \left[1, e^{j2\pi d\cos\theta/\lambda}, \cdots, e^{j2\pi(L-1)d\cos\theta/\lambda}\right]^T \tag{2}$$

where λ is the operation wavelength. d is the sensor distance and usually set as $\lambda/2$ in theoretical analyses. $\boldsymbol{S}(k) = \left[s_0(k), s_1(k), \cdots, s_Q(k)\right]^T$ are the complex envelopes of impacting signals, including potential targets and interferences. It can be assumed that each complex envelope is uncorrelated with each other. $\boldsymbol{N}(k)$ is the noise vector. In most cases, the noise is uncorrelated with any incoming signals, and follows the independent and identical distribution (I.I.D.) condition between different sensors. $[\cdot]^T$ means the transpose operation.

For a regular full-array adaptive beamformer, a minimal variance distortionless response (MVDR) beamformer is usually adopted where the weights come from

$$\boldsymbol{W} = \mu\boldsymbol{R}^{-1}\boldsymbol{a}(\theta_0) \tag{3}$$

scalar μ is the normalized factor. $\mu = \frac{1}{\boldsymbol{a}^H(\theta_0)\boldsymbol{R}^{-1}\boldsymbol{a}(\theta_0})$. $[\cdot]^H$ is the conjugate transpose operator. It makes the beamformer provide unity gain at the desired direction. Then beamforming is achieved by

$$y(k) = \boldsymbol{W}^H\boldsymbol{X}(k) \tag{4}$$

In the real system, the covariance matrix $\boldsymbol{R}$ is always estimated by snapshots with

$$\hat{\boldsymbol{R}} = \frac{1}{K}\sum_{k=1}^{K}\boldsymbol{X}_s(k)\boldsymbol{X}_s^H(k) \tag{5}$$

Here $\boldsymbol{X}_s(k)$ is the chosen K snapshots following the sample matrix inversion (SMI) criterion [24]. The famous CMT method disturbs the estimated covariance matrix to produce wide troughs

$$\hat{\boldsymbol{R}}_T = \hat{\boldsymbol{R}} \odot \boldsymbol{T} \tag{6}$$

Here the operator $\odot$ stands for Hadamard production. The tapering matrix $\boldsymbol{T}$ comes from the famous Mailloux's or Zatman's methods. Using Mailloux's as an example, a cluster of fictitious interferences are assumed around the narrowband interference. Then the tapered covariance matrix becomes

$$\begin{aligned}\left[\tilde{\boldsymbol{R}}\right]_{m,n} &= \sum_{q=1}^{Q} \sum_{p=-(I-1)/2}^{(I-1)/2} \sigma_q^2 e^{j2\pi d(i_n-i_m)(u_q+p\Delta u)/\lambda} + \sigma_N^2 \delta(m,n) \\ &= \sum_{q=1}^{Q} \sigma_q^2 e^{j2\pi d(i_n-i_m)u_q/\lambda} \\ &\quad \cdot \sum_{p=-(I-1)/2}^{(I-1)/2} e^{j2\pi d(i_n-i_m)p\Delta u/\lambda} + \sigma_N^2 \delta(m,n) \\ &= \operatorname{sinc}\left[(i_n - i_m)dW/\lambda\right] \cdot \sum_{q=1}^{Q} \sigma_q^2 e^{j2\pi d(i_n-i_m)u_q/\lambda} \\ &\quad + \sigma_N^2 \delta(m,n) \\ &= [\boldsymbol{R}]_{m,n} \cdot \operatorname{sinc}\left[(i_n - i_m)dW/\lambda\right]\end{aligned} \tag{7}$$

where $[\cdot]_{m,n}$ means the matrix item in the m-th row and n-th column. σ_q^2 is the signal power of the q-th interference. σ_N^2 is the noise power and $\delta(m,n)$ is the 2-D Kronecker function. W is the null width measured in cosine.

Rewriting the sinc function as a matrix, the taper matrix $\boldsymbol{T}$ has the following form

$$[\boldsymbol{T}]_{m,n} = \frac{\sin(m-n)\Delta}{(m-n)\Delta} \tag{8}$$

Here $[\boldsymbol{T}]_{m,n}$ is the m-th row and n-th column element in matrix $\boldsymbol{T}$. Δ is the widening parameter defined in [18]. The taper matrix $\boldsymbol{T}$ describes the correlationship between different sensors from spatial-domain sense [10] or wideband signal sense [11]. Replace $\hat{\boldsymbol{R}}$ in equation (3) with $\hat{\boldsymbol{R}}_T$ and an receiving pattern with wide nulls can be obtained.

III. Flexible Beamforming Method

From the analyses of regular CMT methods, it can be find that all interferences are disturbed identically since the covariance matrix usually contains all interferences. Consequently, the receiving pattern produces all nulls with the same width. Besides, to introduce the wide null into the covariance matrix, Mallioux uses the symmetrical spatial distributed interference cluster [10], while Zatman uses a rectangular spectrum symmetrical to the carrier frequency [11]. Both of these two methods produces symmetrical nulls, so as the following developed methods.

However, in the real system, it is actually not a good idea to produce symmetrical and equal-width mulls. No matter what causes the nonstationarity, the DOA of the source usually varies monotonically and different from each other during the adaption interval. Regular CMT methods must produce wide enough nulls to cover the largest DOA mismatch degree among all nonstationary source and pay two times of DOFs since all wide nulls are symmetrical. It is obviously a great waste of DOFs. Literature [6] proposed a biased CMT-based widening method to overcome the symmetrical null problem. However, its discrete-form solution indeed is not an applicable form.

In this section, we want to handle the two above-mentioned problems under CMT structure. First of all, a continuous form asymmetrical taper matrix will be derived from the Mailloux's methodology which can produce asymmetrical wide nulls. Secondly, based on the prolate spheroidal wave function, an interference matching and eigen-based widening method will be described to widen each null separately. Combining these two steps, the receiving pattern can produce arbitrary width and asymmetrical null for each interference source individually, which achieves totally flexible null widening and saves as many DOFs as possible.

A. Asymmetrically Widening

With Mailloux's methodology, a cluster of fictitious interference sources are put around the original source. However, to produce asymmetrical nulls, at the beginning of the derivation, the fictitious sources are divided into to parts. Under the one-dimentional array model, the two parts of sources are written from $-I_1$ to I_2 instead of regular $-I$ to I where $I_1 \neq I_2$. Then the tapered covariance matrix becomes

$$\begin{aligned}[\boldsymbol{R}_T]_{m,n} &= \sum_{q=1}^{Q} \sum_{p=-I_1}^{I_2} \sigma_q^2 e^{j2\pi d(m-n)(u_q+p\Delta u)/\lambda} + \sigma_n^2 \delta(m,n) \\ &= \sum_{q=1}^{Q} e^{j2\pi d(m-n)u_q/\lambda} \sum_{p=-I_1}^{I_2} \sigma_q^2 e^{j2\pi d(m-n)p\Delta u/\lambda} \\ &\quad + \sigma_n^2 \delta(m,n)\end{aligned} \tag{9}$$

where σ_q^2 is the power of q-th interference. $u_q = \cos\theta$. Δu is the angular spacing between different fictitious interference sources measured in cosine. σ_n is the noise power and $\delta(m,n)$ is the 2-D Kronecker delta function. It can be seen that the first summation presents the regular covariance and the second summation comes from the tapering operation. Now the special tapering matrix $\boldsymbol{T}$ will be derived.

Let the tapering matrix still be $\boldsymbol{T}$, we can obtain

$$\begin{aligned}[\boldsymbol{T}]_{m,n} &= \sum_{p=-I_1}^{I_2} e^{j2\pi d(m-n)p\Delta u/\lambda} \\ &= \frac{e^{-j2\pi d I_1(m-n)\Delta u/\lambda}(1 - e^{j2\pi d(I_1+I_2+1)(m-n)\Delta u/2\lambda})}{1 - e^{j2\pi d(m-n)\Delta u/\lambda}} \\ &= \frac{e^{j2\pi d(m-n)(I_2+1)\Delta u/\lambda} - e^{-j2\pi d(m-n)I_1\Delta u/\lambda}}{e^{j2\pi d(m-n)\Delta u/\lambda} - 1}\end{aligned} \tag{10}$$

With the sum formula of geometric series, we get equation (10). It is a familiar form but different from the regular CMT.

It can also be simplified by Euler's formula

$$[\boldsymbol{T}]_{m,n} = \frac{e^{j2\pi d(m-n)(I_2+I_1+1)\Delta u/2\lambda} - e^{-j2\pi d(m-n)(I_2+I_1+1)\Delta u/2\lambda}}{e^{j2\pi d(m-n)\Delta u/2\lambda} - e^{-j2\pi d(m-n)\Delta u/2\lambda}} \cdot \frac{e^{j2\pi(m-n)(I_2-I_1+1)\Delta u/2\lambda}}{e^{j2\pi d(m-n)\Delta u/2\lambda}} \quad (11)$$

The first part in equation (11) will become a sinc($\cdot$) function [12]. The second part is a phase comes from the asymmetrical widening operation. Following the typical derivations in CMT, $I_1\Delta u = W_1$ and $(I_2+1)\Delta u = W_2$. Then the continuous-form tapering matrix is derived

$$[\boldsymbol{T}]_{m,n} = \mathrm{sinc}((m-n)(W_2+W_1)d/\lambda) \cdot e^{j2\pi d(m-n)(W_2-W_1)/2\lambda} \quad (12)$$

From equation (12), it is obviously that the phase $e^{j2\pi d(m-n)(W_2-W_1)/2\lambda}$ achieves asymmetrical nulls. It means that the asymmetrical tapering matrix contains not only the spatial spreading modulation but also the offset phase. This solution can also be understood from Zatman's view. For a biased frequency spectrum with frequency offset Δf and bandwidth b_ω, it is easy to find that $(W_2 - W_1)/2$ indeed refers to the frequency offset since the null width W is just a normalized frequency [18].

B. Interference Matching and Selective Widening

With the above-mentioned tapering matrix, asymmetrical nulls can be derived. This achieves a part of our goals. In this subsection, the method to widen different null with different width and offset will be discussed. This will achieve our goal of flexibility completely.

CMT-based methods indeed introduce spatial or time-frequency correlationship between different sensors. From equation (9), it points out that the tapering operation is applied to every individual sources

$$\boldsymbol{R}_T = \sum_{q=1}^{Q} \sigma_q^2 \boldsymbol{a}(\theta_q)\boldsymbol{a}^H(\theta_q) \odot \boldsymbol{T} + \sigma_n^2 \mathbf{I} \quad (13)$$

However, it is difficult to obtain the accurate steering vectors in the real system for the imperfect array manifold. To widen different nulls individually, it is key to find the way to recognize different interference sources in snapshots and separate them. In fact, the eigenvectors, or principle components, are good candidates. With existing theories, for a space-time stationary stochastic process, all its first-order and second-order characteristics are contained in the covariance and, at the same time, the eigen-decomposition (discrete Karhunen-Loeve expansion) is the optimal second-order decomposition to transform the stochastic process to a linear combination of a series of normalized and orthogonal bases. Here the constraint of stationarity does not contradict our work since the interference sources in snapshots usually vary little and can be viewed as stationary. This is also the potential assumption of CMT-based methods. The eigen-decomposition operation is

$$\boldsymbol{R} = \sum_{l=1}^{L} \lambda_l \boldsymbol{u}_l \boldsymbol{u}_l^H \quad (14)$$

where λ_l and $\boldsymbol{u}_l$ are the l-th eigenvalue and eigenvector, respectively. Based on the prolate spherical wave function, these eigenvalues and eigenvectors have deterministic linear relationship [17].

$$\boldsymbol{u}_l = c_{1l}\boldsymbol{a}(\theta_1) + c_{2l}\boldsymbol{a}(\theta_2) + \cdots + c_{Ql}\boldsymbol{a}(\theta_Q) \quad (15)$$

Here $l = 1, 2, \cdots, Q$ and the parameter c_{ql} is the coefficient depends on the time-domain and spatial mutual correlationship between different sources. These eigenvectors consist of the so-called "signal subspace". Other $L - Q$ eigenvectors span the noise subspace. These two subspaces can be recognized by the varying trend of corresponding eigenvalues [25]. More importantly, for separated uncorrelated sources, each eigenvector in the signal subspace mainly stands for a certain steering vector. Taking the case with two equal-power and uncorrelated sources as an specific example, the two eigenvectors in the subspace are

$$\boldsymbol{u}_{1(2)} = \frac{\boldsymbol{a}(\theta_1) \pm e^{-j\phi(\rho_c^{12})}\boldsymbol{a}(\theta_2)}{\sqrt{2L(1 \pm |\rho_c^{12}|)}} \quad (16)$$

In equation (16), ρ_c^{12} represents the spatial correlationship between these two sources. For an uniform linear array, the ρ_c^{12} comes from the $sinc$ function

$$\rho_c^{12} = \frac{\boldsymbol{a}^H(\theta_1)\boldsymbol{a}(\theta_2)}{L} \approx \frac{sin(L(\theta_1-\theta_2)\pi/2)}{L(\theta_1-\theta_2)\pi/2} \quad (17)$$

Operation $\phi(\cdot)$ calculate the phase of the object. From equation (16), it is obviously that the eigenvector in the signal subspace consists of two steering vectors. The farther apart two sources are, the more similar each eigenvector is to the corresponding steering vector since ρ_c^{12} becomes smaller. For a general case that more than two interference sources impacting on the array, this correspondence still exists. It still can find a certain eigenvector for a corresponding sources but is hard to be expressed as such a simple form as equation (16).

With this important solution, a flexible way that can widen each null individually is derived. For a eigen-decomposed covariance, the widening is applied to each eigenvector.

$$\boldsymbol{R}_T = \sum_{l=1}^{Q} \lambda_l \boldsymbol{u}_l \boldsymbol{u}_l^H \odot \boldsymbol{T}_l + \sum_{l=Q+1}^{L} \lambda_l \boldsymbol{u}_l \boldsymbol{u}_l^H + \gamma \mathrm{I}_L \quad (18)$$

where $\boldsymbol{T}_l$ is the corresponding tapering matrix. $\gamma \mathrm{I}_L$ is a diagonal loading item to make the sidelobe stable. In most cases, this diagonal loading operation is necessary to insure nonsingularity since the selective widening will disturb the noise-subspace slightly [26]. Here we try to give some analyses from our point of view. From equation (6) and (13), it can be seen that regular tapering matrix is applied to the whole covariance matrix. Since the main diagonal elements of the tapering matrix $\boldsymbol{T}$ equals to 1, equation (6) is equivalent to equation (13). However, the selective widening operation will change the distribution of the signal and noise subspace, resulting in singularity. The influence that the proposed method takes on the noise subspace can be illustrated with a widening procedure with identical tapering matrix.

$$\begin{aligned} \boldsymbol{R}_T &= \sum_{l=1}^{Q} \lambda_l \boldsymbol{u}_l \boldsymbol{u}_l^H \odot \boldsymbol{T} + \sum_{l=Q+1}^{L} \lambda_l \boldsymbol{u}_l \boldsymbol{u}_l^H \\ &= \left(\sum_{l=1}^{Q} \lambda_l \boldsymbol{u}_l \boldsymbol{u}_l^H + \sum_{l=Q+1}^{L} \lambda_l \boldsymbol{u}_l \boldsymbol{u}_l^H \odot \tilde{\boldsymbol{T}} \right) \odot \boldsymbol{T} \end{aligned} \tag{19}$$

The first part comes from interferences and noise. The second part comes from the noise. $\tilde{\boldsymbol{T}} \odot \boldsymbol{T} = \mathbf{1}$. $\mathbf{1}$ is a matrix with all ones in it. Compared with the regular CMT that tapering all the covariance matrix, the proposed method only tapers the selective principle components. The second row of equation (19) shows that the proposed method can be viewed as a regular tapering applied to a modified covariance with disturbed noise subspace. The disturbed noise subspace will indeed lead to fluctuating sidelobes. When tapered with different matrix, this explanation also holds. This is the reason why we must use diagonal loading to get a stable array pattern. With loading, the disturbed noise subspace returns to stable and tapering information is still perserved.

However, too much loading will make the null depth distorted. Fortunately, only a small loading factor γ is enough. This makes the proposed method still suitable for application since diagonal loading is a regular operation in the real system. A corresponding experiment is given in the next section to show this performance.

C. Complete Procedure and Some Discussions

Based on the above-mentioned two flexible widening steps, the main body of our work has been established. However, some necessary steps cannot be ignored, including nonstationarity estimating and eigenvector matching. In this subsection, we will complete the whole scheme and make some discussions.

The nonstationarity is one of the most important parameters in null widening methods. In real systems, DOA estimation methods are a straightforward way. Systems can adopt APES or MUSIC methods periodly to track the nonstationary variation of the interference DOA. Taking radar as an example, system can estimate the DOA at the end of each pulse repetition interval (PRI) in the sector that existing interferences. Estimating results can show the nonstationarity within each adaption interval. Besides, some specific method for nonstationary DOA estimation was proposed [27] which can obtain the time-varying DOA directly. It must be pointed out that the movement of the platform can be predicted. If systems cannot achieve DOA estimation, this information will become a good indication for nonstationarity. The mechanical rotation of the radar receiving array is a typical example.

The eigenvector matching is another important step in the whole scheme. As the above-mentioned analyses, each eigenvector indeed comes from a certain steering vector in the separated source scene. Based on the orthogonality between different steering vector, a matching procedure is adopted. With DOA estimation results, the relatively precious steering vector can be reconstructed $\boldsymbol{a}(\hat{\theta}_1), \boldsymbol{a}(\hat{\theta}_2), \cdots, \boldsymbol{a}(\hat{\theta}_Q)$. After eigen-decomposition, each eigenvector in the "signal" subspace will be projected to the reconstructed steering vectors.

$$\underset{\hat{\theta}_q}{argmax}\, |\boldsymbol{a}^H(\hat{\theta}_q)\boldsymbol{u}_l| \tag{20}$$

With the searching procedure, each interference can find its corresponding eigenvector. This matching result can be substituted into equation (13). Then the widening operation can be achieved on eigenvectors instead of ideal steering vector that cannot derived in real systems.

Until now, all necessary steps have been established. The complete flexible null widening method is concluded as follows.

Algorithm 1 Algorithm Procedure of the Proposed Null Widening Method.

Require: The snapshots of received data, $\boldsymbol{x}_{(k)}$; The widening random variable, $\boldsymbol{W}_{opt}$;

Ensure: Adaptive weights, $\boldsymbol{W}_{opt}$;

1: Estimate the DOA of interference sources in snapshots and their nonstationarities, respectively.

2: Set necessary null width for each interferences, recording as $[-W_{q,1}, W_{q,2}]$.

3: Construct tapering matrix with each null width using equation (12).

4: Decompose the covariance matrix to obtain principle components of all eigenvalues.

5: Match each eigenvalue of principle components with reconstructed steering vector with equation (20).

6: Widen each matched eigenvalue with corresponding taper matrix to obtain tapered covariance matrix in equation (18).

7: Produce beamformer $\boldsymbol{\omega}$ using MVDR algorithm where covariance matrix is replaced by $\boldsymbol{R}_T$.

8: **return** $\boldsymbol{W}_{opt}$;

With these steps, a flexible widening beamformer is achieved. Here some discussions will be given.

Firstly, in the above-mentioned contents, it is assumed that all the interference sources are spatially separated. This assumption will lead to a good performance of the proposed method. However, if several uncorrelated sources are crowded and impact on the array with similar DOA occasionally, the proposed method also holds. In this case, corresponding subspaces will spread. The matching relationship will suffer a little loss. To cover this situation, the matching step can be modified as

$$\underset{\hat{\theta}_q}{\text{argmax}}\, |\boldsymbol{a}^H(\hat{\theta}_q)\boldsymbol{u}_l| \tag{21}$$

$$s.t. |\boldsymbol{a}^H(\hat{\theta}_q)\boldsymbol{u}_l| > \eta \tag{22}$$

Here η is the normalized relationship threshold. It can be set as 0.5. With this modification, this step can find out separated sources. For the left eigenvectors, they can be viewed as crowded sources and be widened together to procedure a wider null covering all the crowded sources.

Secondly, it should be pointed out that why the eigenvectors are used to achieve separated widening operation

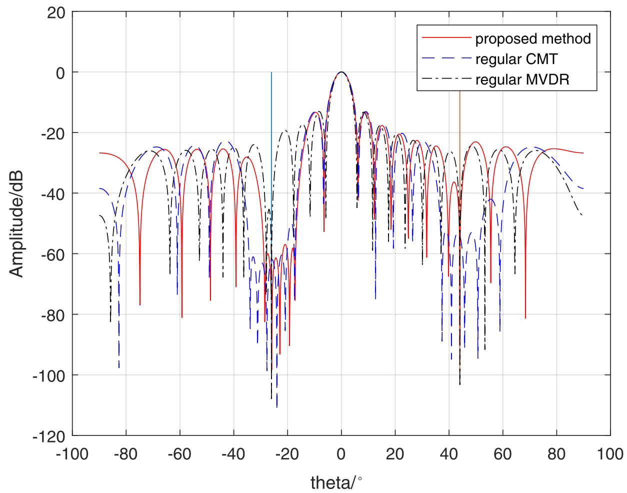

Fig. 2. Pattern comparison for single null widening.

instead of reconstructed steering vectors. In the real system, the array always contains unavoidable errors. However, the reconstructed steering vectors use the idea array manifold. But the eigenvectors come from snapshots, which contain information of the real array. As a result, eigenvectors are chosen to achieve the key step and reconstructed steering vectors are just used to estimate the correlation, which is not sensitive to the manifold errors.

IV. Simulation Results

In this section, some simulation results are provided to show the effectiveness of the proposed method. The adaptive array is set as follows. A linear array with 20 omni-directional sensors are considered. The target of interests comes from 0°. Two interferences come from $-26°$ and 44°, respectively. The interference-to-noise ratios (INR) are $30dB$ and $20dB$, respectively. For comparison, the regular MVDR and CMT are also simulated. For regular CMT, the widening factor Δ is set as 0.2. For the proposed method, the width is divided into 0.05 and 0.15.

A. Single Null Widening

In this section, the ability of single null widening is evaluated, compared with MVDR and regular CMT, i.e. Mailloux's method. Here the left width is chosen as 0.05 and right width is chosen as 0.15. Adaptive pattern is shown in fig. 2.

From this figure, the classical MVDR method produces two sharp nulls in the corresponding direction. It is clear that sharp nulls cannot afford nonstationary interference cancellation. For the regular CMT method, two wide nulls are produced with symmetric width around the central direction. However, this widening operation wastes some DOFs in real systems since most of nonstationary interferences have specific motion direction and do not need symmetric widened nulls, even just needing sharp nulls. To show the effectiveness of the selective widening of the proposed method, the interference impacting from $-26°$ is chosen to widen an asymmetric null. From the pattern, it can be seen that the null at the chosen direction becomes a widen null and is skewed to the right side, resulting from the asymmetric widening parameters. On the other side,

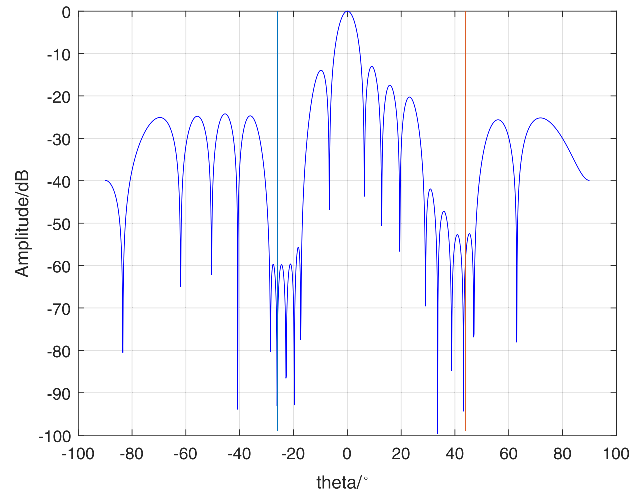

Fig. 3. Adaptive pattern for flexible null widening.

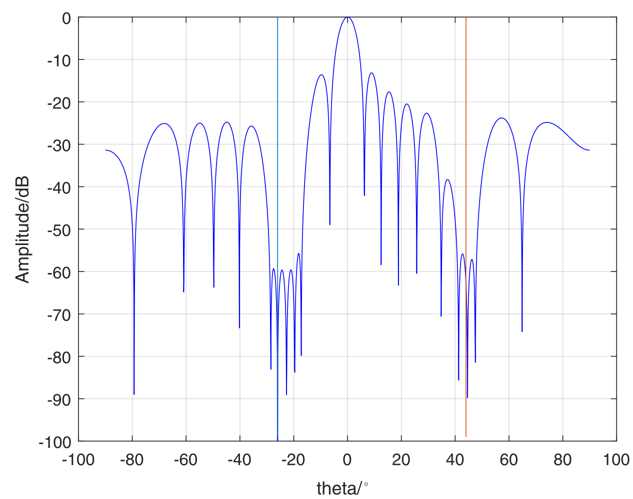

Fig. 4. Adaptive pattern for flexible null widening with different width.

the interference at 44° maintains a sharp null. This adaptive pattern verifies that the proposed method can achieve single null asymmetric widening.

B. Flexible Null Widening

In this experiment, the flexibility of the proposed method will be further verified. Two interference sources are set as different asymmetric nulls. The interference impacting from $-26°$ is set as 0.05 at left and 0.15 at right, and the other interference is just the reverse. The adaptive pattern is shown in Fig. 3.

It is obviously that the proposed method successfully achieves different deviation for different null. The interference at $-26°$ produces an asymmetric null that is skewed to the positive axis, just as in Fig. 2. On the contrary, the null at 44° becomes a wide null which is skewed to the negative axis. This result corroborates the flexibility of the proposed method, which is the deep motivation of our work.

For more complicated case, the pattern can also achieve pattern with different widths and different deviations. In Fig. 4, we set the null at 44° as a symmetric wide null with width 0.1. The proposed method also achieves the goal. An asymmetric

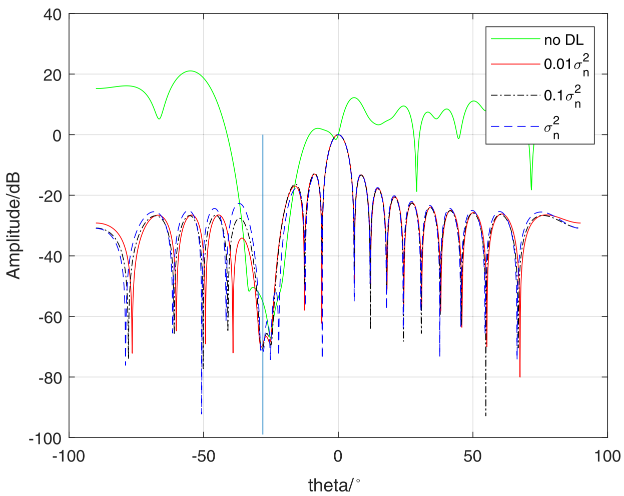

Fig. 5. Diagonal loading test with different factor values.

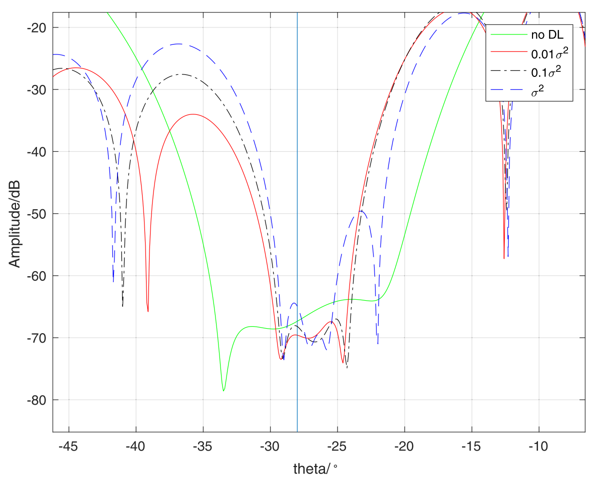

Fig. 6. Close-up widen null of different loading factor values.

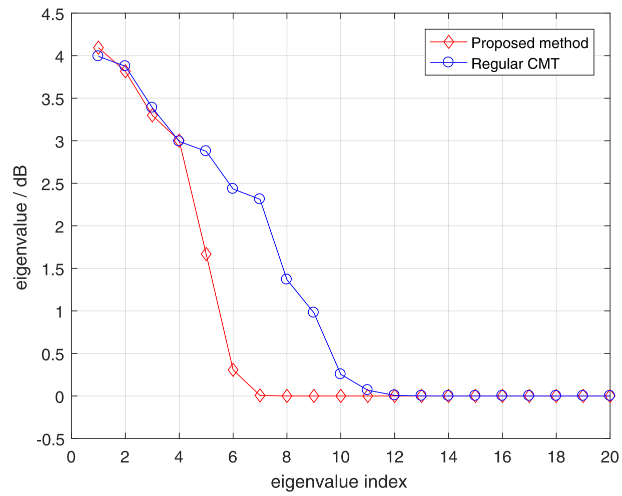

Fig. 7. DOF comparison between proposed method and regular CMT.

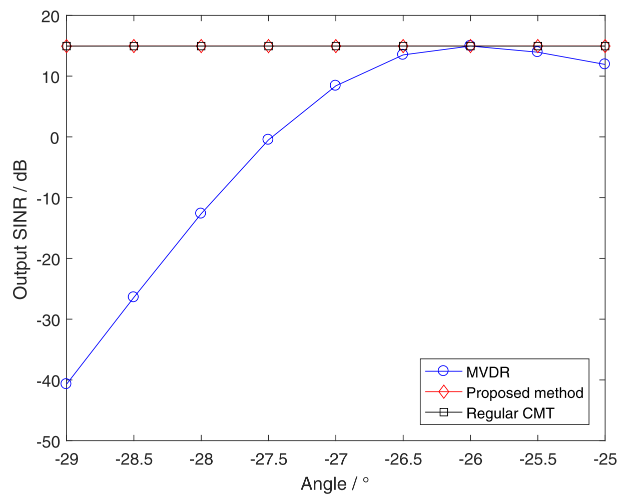

Fig. 8. Output SINR comparison between MVDR, proposed method and regular CMT.

null at $-26°$ and symmetric null at $44°$ with different width are produced.

C. Diagonal Loading Test

In this experiment, the stability of the sidelobe and diagonal loading are tested. The diagonal loading factor is measured as the simulated noise power σ_n^2. To analyze the effects of the loading quantity, loading factor of $0, 0.01\sigma_n^2, 0.1\sigma_n^2, \sigma_n^2$ are simulated. Results are shown in Fig. 5. To make the results more clearer, a close-up shot is also given in Fig. 6.

From the result, it is obvious that the proposed method will fluctuate the sidelobe and make the pattern unavailable. With diagonal loading increasing, the pattern returns to normal rapidly. At the same time, the larger the loading factor uses, the more stable the sidelobe is. On the other side, the null depth become shallower with loading factor increasing, even the factor is as small as $0.01\sigma_n^2$. Therefore, the conclusion can be drawn that the diagonal loading is necessary, but a small loading factor is enough for the procedure since the widening effect has become effective from the very beginning.

D. DOF Costs Test

A simulation of DOF comparison is shown in Fig.7. In this simulation, the necessary null width is biased which needs left width factor 0.10 and right width factor 0.05. The proposed method is widened as necessary. However, to cover the varying DOA, regular CMT method needs to widen a null with width factor 0.2.

It can be seen that the proposed method saves about 6 DOFs compared with regular CMT method, i.e. each wide null 3 DOFs. This result corroborates that our work indeed achieves the major goal successfully. The reason is that the proposed method can adjust each wide null with desired nonstationarity, while the regular CMT method must widen each null with equal and maximum null width.

E. Output SINR

In this experiment, the beamforming output signal-to-noise ratio (SINR) is evaluated to show the effectiveness of the proposed method using Monte Carlo method. The Monte Carlo number is set as 1000. To make the results clearer, only one interference with 40 dB interference-to-noise ratio is simulated. During the processing interval, the DOA of the interference varies from $-29°$ to $-25°$. Ideal signal-to-noise ratio is assumed as 15 dB. The MVDR, regular CMT and the proposed method are all evaluated. It is suppose that the MVDR method chooses a small group of snapshots to training beamformer where the DOA of the interference within snapshots is close to $-26°$. It can be inferred that the MVDR will suffer performance loss since it cannot generate a wide null.

As Fig. 8 shown, the regular CMT and the proposed method achieve interference cancellation successfully, while the MVDR fails. Since the nonstationarity is not asymmetric, the output SINR in angle $-29°$ is much lower than that in angle $-25°$. The reason is obvious that the regular CMT and proposed method widen the null. However, the regular CMT must widen the null to the maximum width, which will waste DOFs. Considering the last experiment, the performance and advantages of the proposed method are self-evident.

V. Conclusion

Covariance matrix tapering is an effective way to cancel nonstationary interference at beamforming stage. However, the nonstationarity of different interferences can hardly be identical to each other. This will result in a wasting of DOFs since existing CMT methods produce the same null width to all nulls. In this paper, based on the match relationship between principle components and steering vectors, a flexible CMT-based null widening method is proposed. It can achieve asymmetrical wide null with different width for different null by tapering different principle component with different asymmetrical taper matrix. Simulation results show that the proposed method can achieve the flexible widening goal. Compared with regular methods, it provides a flexible option for the real system.

References

[1] C. Zhou, Y. Gu, S. He, and Z. Shi, "A robust and efficient algorithm for coprime array adaptive beamforming," *IEEE Trans. Veh. Technol.*, vol. 67, no. 2, pp. 1099–1112, Feb. 2018.

[2] X. Wang, M. Amin, and X. Cao, "Analysis and design of optimum sparse array configurations for adaptive beamforming," *IEEE Trans. Signal Process.*, vol. 66, no. 2, pp. 340–351, Jan. 2018.

[3] J. Shi *et al.*, "Transmit design for airborne MIMO radar based on prior information," *Signal Process.*, vol. 128, pp. 521–530, Nov. 2016.

[4] G. A. Fabrizio, Y. I. Abramovich, S. J. Anderson, D. A. Gray, and M. D. Turley, "Adaptive cancellation of nonstationary interference in HF antenna arrays," *IEE Proc. Radar Sonar Navigat.*, vol. 145, no. 1, pp. 19–24, Feb. 1998.

[5] Z. Liu, H. Su, and Q. Hu, "Transient interference suppression for high-frequency skywave over-the-horizon radar," *IET Radar, Sonar Navigat.*, vol. 10, no. 8, pp. 1508–1515, Oct. 2016.

[6] Y. Cao, Y. Guo, S. Liu, and Y. Liu, "Adaptive null broadening algorithm based on sidelobes cancellation," *J. Electron. Inf. Technol.*, vol. 42, no. 3, pp. 597–602, 2020.

[7] S. Wu, J. Zhang, and S. Zhang, "Research on beamforming of wide nulling algorithm," *J. Harbin Eng. Univ.*, vol. 25, no. 5, pp. 658–661, 2004.

[8] F. Liu, C. Sun, and J. Wang, "Nulls control method based on semidefinite programming," *J. Northeastern Univ., Natural Sci.*, vol. 32, no. 10, pp. 1386–1389, 2011.

[9] Z. Fan, G.-L. Liang, and Y.-L. Wang, "Robust adaptive beamforming with null widening," *J. Electron. Inf. Technol.*, vol. 35, no. 11, pp. 2764–2770, Feb. 2014.

[10] R. J. Mailloux, "Covariance matrix augmentation to produce adaptive array pattern troughs," *Electron. Lett.*, vol. 31, no. 10, pp. 771–772, May 1995.

[11] M. Zatman, "Production of adaptive array troughs by dispersion synthesis," *Electron. Lett.*, vol. 31, no. 25, pp. 2141–2142, Dec. 1995.

[12] J. R. Guerci, "Theory and application of covariance matrix tapers for robust adaptive beamforming," *IEEE Trans. Signal Process.*, vol. 47, no. 4, pp. 977–985, Apr. 1999.

[13] R. Li, Y. Wang, and S. Wan, "Research on adaptive pattern null widening techniques," *Mod. Radar*, vol. 25, no. 2, pp. 42–45, 2003.

[14] G. Liang, B. Han, and Z. Fan, "Null broadening of near-field adaptive beamforming," *J. Huazhong Univ. Sci. Technol., Natural Sci. Ed.*, vol. 41, no. 8, pp. 34–39, 2013.

[15] Z. Li, J. You, and X. Cai, "Nulling broadening technology based on circular array adaptive beamforming," in *Proc. IEEE 14th Int. Conf. Commun. Technol.*, Nov. 2012, pp. 1123–1128.

[16] K. Buckley, "Spatial/spectral filtering with linearly constrained minimum variance beamformers," *IEEE Trans. Acoust., Speech, Signal Process.*, vol. 35, no. 3, pp. 249–266, Mar. 1987.

[17] D. Slepian and H. O. Pollak, "Prolate spheroidal wave functions, Fourier analysis and uncertainty—I," *Bell Syst. Tech. J.*, vol. 40, no. 1, pp. 43–63, Jan. 1961.

[18] H. Su, H. Liu, P. Shui, and Z. Bao, "Adaptive beamforming for nonstationary HF interference cancellation in skywave over-the-horizon radar," *IEEE Trans. Aerosp. Electron. Syst.*, vol. 49, no. 1, pp. 312–324, Jan. 2013.

[19] Z. Yang, R. C. de Lamare, and X. Li, "L_1-regularized STAP algorithms with a generalized sidelobe canceler architecture for airborne radar," *IEEE Trans. Signal Process.*, vol. 60, no. 2, pp. 674–686, Feb. 2012.

[20] Z. Liu, H. Su, and Q. Hu, "Robust sidelobes cancellation algorithm with null broadening," *J. Electron. Inf. Technol.*, vol. 38, no. 3, pp. 565–569, 2016.

[21] D. Chapman, "Partial adaptivity for the large array," *IEEE Trans. Antennas Propag.*, vol. 24, no. 5, pp. 685–696, Sep. 1976.

[22] E. Brookner and J. M. Howell, "Adaptive-adaptive array processing," *Proc. IEEE*, vol. 74, no. 4, pp. 602–604, Apr. 1986.

[23] R. Li, S. Zhao, and L. Dai, "An adaptive-adaptive beamforming algorithm with nulls widening," in *Proc. 2nd Int. Congr. Image Signal Process.*, Oct. 2009, pp. 1–5.

[24] I. S. Reed, J. D. Mallett, and L. E. Brennan, "Rapid convergence rate in adaptive arrays," *IEEE Trans. Aerosp. Electron. Syst.*, vol. AES-10, no. 6, pp. 853–863, Nov. 1974.

[25] J. A. Cadzow and Y. S. Kim, "General direction-of-arrival estimation—A signal subspace approach," *IEEE Trans. Aerosp. Electron. Syst.*, vol. 25, no. 1, pp. 31–47, Jan. 1989.

[26] J. R. Guerci and J. S. Bergin, "Principal components, covariance matrix tapers, and the subspace leakage problem," *IEEE Trans. Aerosp. Electron. Syst.*, vol. 38, no. 1, pp. 152–162, Aug. 2002.

[27] D.-C. Chang and B.-W. Zheng, "Adaptive generalized sidelobe canceler beamforming with time-varying direction-of-arrival estimation for arrayed sensors," *IEEE Sensors J.*, vol. 20, no. 8, pp. 4403–4412, Apr. 2020.